Int. J. Heat Mass Transfer. Vol. 29, No. 8, pp. 1237–1244, 1986
Printed in Great Britain

0017-9310/86 $3.00+0.00
Pergamon Journals Ltd.

Radiation-induced ignition of condensed fuels in a ceiling fire including effects of radiation blockage

K. Y. LEE* and C. L. TIEN
Department of Mechanical Engineering, University of California, Berkeley, CA 94720, U.S.A.

Abstract—Effects of thermal radiation blockage due to an absorbing–emitting layer formed below the ceiling on ignition of the floor materials are studied. The analysis employs a relatively simple but realistic model under one-dimensional and quasi-steady-state conditions. Calculated ignition delay times compare favorably with experimental data and temperature histories of the floor influenced by radiation blockage are obtained. Generally valid relationships between ignition delay times and radiative heat fluxes are obtained for typical polymer fuels such as PMMA and PS, and the applicability of the present analysis is discussed.

1. INTRODUCTION

IN ROOM or compartment fires, since thermal radiation is a dominant mode of heat exchange [1, 2], ignition by radiative heat input is of great practical importance in association with the assessment of fire hazards. Radiative heat feedback from the flames may often be sufficient to ignite remote combustible objects such as floors and carpets. Ignition by these remote sources may be distinguished from the initiating ignition by foreign sources such as cigarettes. In an enclosure fire with somewhat restricted ventilation, a smoke layer of strongly participating combustion products such as soot particles at a high temperature is often formed below the ceiling. Due to the strongly absorbing nature of the smoke layer, radiative heat feedback from the flame is substantially attenuated; this is referred to as blockage or blanketing of thermal radiation.

Radiation blockage due to the layer of decomposition products has recently drawn particular research attention. Kashiwagi investigated this effect on ignition characteristics of PMMA and red oak [3]. Using empirical correlations, he successfully compared the fuel surface temperature histories and ignition delay times with the experimental data. However, his analysis is applicable only when the empirical correlations of timewise variation of heat fluxes are known, and thus, can not generally be applied to other fuels. The present study attempts to generalize Kashiwagi's work by introducing radiation blockage into the analysis. Since blockage is dependent only on thermophysical and radiative properties of fuels or systems, it may serve as a well-defined parameter in the calculation of radiative heat attenuation [4]. The aim of present study is to investigate the effect of radiation blockage due to the smoke layer on the ignition characteristics of reactive floor materials. For this purpose, surface temperature histories for various heat fluxes as well as ignition delay times are to be obtained as a function of radiative heat fluxes. Improved understanding of the heat exchange process in a room fire may lead to a better planning of safety measures such as evacuation, and thus is very important in many practical applications.

2. ANALYTIC MODEL AND FORMULATION

2.1. *Description of model and assumptions*

Figure 1 represents the idealized ceiling fire situation which is analyzed in this work. A semi-infinite solid fuel (floor) subject to radiative heating on the surface through the smoke is studied. For simplicity, heat exchange in the gas layer is assumed to be one-dimensional and in radiative equilibrium. Since the

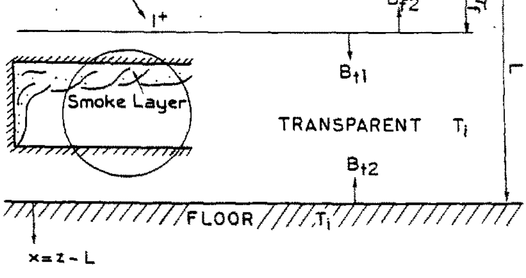

FIG. 1. Schematic of the system for radiative ignition in a ceiling fire.

---

* Present address: Department of Mechanical and Aerospace Engineering, West Virginia University, Morgantown, WV 26506, U.S.A.

NOMENCLATURE

A	dimensionless parameter, equation (26)
B	radiosity or heat flux [kW m^{-2}]
C_s	dimensionless heat source intensity, $(S/k)/(B_{f1}-B_{f2})$
c	specific heat [kJ kg^{-1} K^{-1}]
E	activation energy [kJ mole^{-1}]
$E_n(t)$	exponential integral of order n, $\int_0^1 \mu^{n-2}\exp(-t/\mu)\,\mathrm{d}\mu$
H	head of combustion [kJ kg^{-1}]
h	convective heat transfer coefficient [kW m^{-2} K^{-1}]
I	intensity of radiation [kW m^{-2}]
k	absorption coefficient [m^{-1}]
L	smoke layer thickness [m]
Q	dimensionless heat flux, $q_R/(B_{f1}-B_{f2})$
q	heat flux [kW m^{-3}]
R	universal gas constant, 8.3143 kJ kmol^{-1} K^{-1}
S	volumetric heat source intensity [kW m^{-3}]
T	temperature [K]
t	time [s]
x, z	position coordinate [m].

Greek symbols

α	thermal diffusivity [m^2 s^{-1}]
β	blockage of thermal radiation, equation (13)
ε	emissivity
θ	dimensionless temperature, $(T-T_i)/T_i$
λ	thermal conductivity [kW m^{-1} K^{-1}]
ν	frequency factor [s^{-1}]
σ	Stefan–Boltzmann constant, 5.6696×10^{-11} kW m^{-2} K^{-4}
τ	optical coordinate, $\int_0^z k(y)\,\mathrm{d}y$
ϕ	dimensionless temperature, $(\sigma T^4-B_{f2})/(B_{f1}-B_{f2})$
$\phi_s(\tau)$	dimensionless source function, equation (8).

Subscripts and Superscripts

f	smoke layer
i	initial
ig	ignition
s	solid fuel
w	ceiling
*	dimensionless.

thermal diffusivity of the gas is 2 or 3 orders of magnitude greater than that of the solid, the quasi-steady approximation appears to be reasonably adequate for the analysis [5]. It is also assumed that the radiative heat is absorbed at the surface. Even when the in-depth absorption of radiation heat is considered, the analysis becomes identical to the lowest order. This point will be subsequently discussed in detail. Scattering by soot particles is neglected and thermophysical properties, such as the thermal conductivity, and radiative properties, such as the absorption coefficient, are assumed to be constant and wavelength independent. The temperature of the ceiling is fixed at the pyrolyzing temperature and the average gas temperature of the smoke layer is taken as the effective flame radiation temperatures: 1538 K for PMMA and 1732 K for red oak [6]. This temperature is used in the calculation of the average absorption coefficient of the ceiling layer. The gas layer thickness is approximated to be constant, since a short time after a fire, it becomes nearly constant due to the balancing effect of ventilation through windows or doorways [2]. The region beyond the smoke layer is assumed to be transparent, only to emphasize that the radiation contribution is small and gas-phase conduction is not included.

2.2. *Formulation for the smoke layer*

The energy equation of the system in radiative equilibrium is given by

$$\frac{\mathrm{d}q_R}{\mathrm{d}z} = S \tag{1}$$

where S denotes the volumetric heat source intensity (kW m^{-3}) due to chemical reactions. For the ceiling layer region far away from the tip of the flame, where no chemical reactions take place, the RHS of equation (1) vanishes. The radiative heat flux, q_R, is found from the solution of the transfer equation as

$$q_R(\tau) = 2B_{f1}E_3(t)-2B_{f2}E_3(\tau_f-\tau) + 2\sigma\int_0^{\tau} T^4(t)E_2(\tau-t)\,\mathrm{d}t - 2\sigma\int_0^{\tau_f} T^4(t)E_2(t-\tau)\,\mathrm{d}t. \tag{2}$$

Differentiating equation (2) twice with respect to τ yields

$$2\sigma T^4 = B_{f1}E_2(\tau)+B_{f2}E_2(\tau_f-\tau) + \sigma\int_0^{\tau_f} T^4(t)E_1(|\tau-t|)\,\mathrm{d}t. \tag{3}$$

Introducing dimensionless temperature

$$\phi(\tau) \equiv (\sigma T^4 - B_{f2})/(B_{f1} - B_{f2}),$$

and heat flux $Q(\tau) \equiv q_R/(B_{f1} - B_{f2})$, respectively, and combining equations (1)–(3) gives

$$\frac{dQ}{d\tau} = C_s \tag{4}$$

where C_s is defined as $(S/k)/(B_{f1} - B_{f2})$, which is the dimensionless heat source intensity. Integral equations (2) and (3) can be approximately solved using the well-known kernel substitution technique. Approximating $E_2(t)$ and $E_3(t)$ as $(3/4)\exp(-3t/2)$ and $(1/2)\exp(-3t/2)$, respectively, then equation (3) is reduced to a first-order differential equation by differentiating it twice

$$\phi'(\tau) = -\frac{3}{4}Q. \tag{5}$$

Combining equations (4) and (5), the temperature and heat flux are found, after some algebraic manipulation, to be

$$\phi(\tau) = \left(1 - \frac{1/2}{1+3\tau_f/4} - \frac{3\tau/4}{1+3\tau_f/4}\right) + C_s\phi_s(\tau) \tag{6}$$

$$Q(\tau) = \frac{1}{1+3\tau_f/4} + C_s(\tau - \tau_f/2) \tag{7}$$

where $\phi_s(\tau)$ is a dimensionless source function and is given by

$$\phi_s(\tau) = 3\tau(\tau_f - \tau)/8 + \tau_f/4 + 1/3. \tag{8}$$

The boundary conditions of the equation of transfer are given by

$$q_R(0)\left(\frac{1}{\varepsilon_1} - 1\right) = \sigma T_w^4 - B_{f1} \tag{9}$$

$$q_R(\tau_f)\left(\frac{1}{\varepsilon_2} - 1\right) = B_{f2} - \sigma T_i^4. \tag{10}$$

Using the result of equation (7), $(B_{f1} - B_{f2})$ can be found as

$$B_{f1} - B_{f2} = \frac{\sigma(T_w^4 - T_i^4) + (\tau_f S/2k)(1/\varepsilon_1 - 1/\varepsilon_2)}{\{1 + [1/(1+3\tau_f/4)]\}(1/\varepsilon_1 + 1/\varepsilon_2 - 2)}. \tag{11}$$

If no chemical reactions take place in the ceiling layer, i.e. $S = 0$, then equation (11) reduces to the same expression as found in ref. [7]. Also, if both the ceiling and floor are black, $(B_{f1} - B_{f2})$ becomes simply $\sigma(T_w^4 - T_i^4)$, as should be expected. Radiative flux at the edge of the smoke layer, $q_R(\tau_f)$ is important in the ignition calculation. From equation (10), $q_R(\tau_f)$ is found as

$$q_R(\tau_f) = \left(\frac{1}{1+3\tau_f/4}\right) \times \left\{\frac{\sigma(T_w^4 - T_i^4) + (\tau_f S/2k)(1/\varepsilon_1 - 1/\varepsilon_2)}{[1/(1+3\tau_f/4)](1/\varepsilon_1 - 1/\varepsilon_2 - 2)}\right\} + \frac{\tau_f S}{2k}. \tag{12}$$

Radiation blockage, β, measures the fraction of radiative heat attenuation due to the presence of the participating medium. Thus, it can be defined as

$$\beta = 1 - \frac{\pi I(0)}{\pi I(\tau_f)} = 1 - \frac{q_{net}(0)}{q_{net}(\tau_f)}. \tag{13}$$

Net radiative heat flux between two infinite parallel plates is given by

$$q_{net} = \frac{\sigma(T_w^4 - T_i^4)}{1/\varepsilon_1 + 1/\varepsilon_2 - 1}. \tag{14}$$

As a simple case of no chemical reaction ($S = 0$), from equations (12) and (14), radiation blockage can be found as

$$\beta = \frac{3\tau_f/4}{3\tau_f/4 + 1/\varepsilon_1 + 1/\varepsilon_2 - 1}. \tag{15}$$

If chemical reactions occur in the ceiling layer, radiation blockage becomes dependent on both T_i and T_w. With the assumption that the chemical reactions take place at an infinitely fast rate, and that the ceiling surface is black, it can be shown that

$$\beta = \frac{3\varepsilon_s\tau_f/4}{1+3\varepsilon_s\tau_f/4}[1 - (T_i/T_w)^4]. \tag{16}$$

From equation (16), it can be noted that the blockage effect is not sensitive to T_i/T_w values, as long as T_i is much less than the flame temperature. Since the fuel surface temperature is close to the ambient temperature before ignition has occurred, the approximation of constant β will not lead to a significant error for the smoke layer analysis even for the cases of chemical reactions.

2.3. *Formulation for the solid fuel*

Ignition mechanisms of polymeric fuels are not yet clearly understood. Recent experimental studies, however, show that the ignition delay of polymers is primarily governed by the induction period of pyrolyzed gas reactions close to the fuel surface [8]. For solid propellant ignition, the exothermic surface gasification can facilitate the ignition process, while in the ignition of polymers, the endothermic nature of fuel pyrolysis may suppress the ignition process, yielding relatively longer ignition delays as a consequence [9]. Interpreting polymer fuel ignition mechanisms by adopting the theory of solid propellant ignition can possibly result in shorter ignition delay times than the actual values. The theoretical analysis of Kashiwagi [10] shows, however, that the endothermicity of fuel pyrolysis is of minor importance in determining ignition delay times. Hence, reasonably accurate predictions are expected to be obtained by using the existing solid fuel ignition theory.

In this theory, chemical reactions in the solid are often ignored for a lower-order analysis, thus the simple heat conduction equation is obtained

$$\frac{\partial T}{\partial t} = \alpha\frac{\partial^2 T}{\partial x^2} \tag{17}$$

where the position coordinate x is defined as $x = z - L$. Boundary and initial conditions are

$$T = T_i \quad \text{at} \quad t = 0 \quad \text{and} \quad x \to \infty \tag{18a}$$

$$\lambda \frac{\partial T}{\partial x} + \varepsilon_s q_R = h(T - T_i) \quad \text{at} \quad x = 0. \tag{18b}$$

Radiative irradiation, the second term in equation (18b), is dependent on both the absorption characteristics of the floor material and the nature of the radiation source. For the typical polymer fuels such as PMMA, it is known that for wavelengths greater than 2.5 μm, the total absorption is above 0.95, whereas in the range of 0.4–1.6 μm, it is a very poor absorber [11]. Assuming the average temperature of the smoke layer below the ceiling is 1100–1500 K, the emission wavelength from the layer lies between 2 and 3 μm according to the Wien displacement law. Also the total emissivity of wood is generally greater than 0.9. This fact allows the approximation of unit emissivity of the floor materials in practical combustion situations of a room fire. During the ignition delay period, the convective heat transfer coefficient, h, tends to decrease with time mainly because convection becomes less effective with an increase of the fuel surface temperature [8]. At the beginning of heating, this decrease is sharp, but due to the build-up of pyrolyzed gases close to the surface, the decrease becomes slower with time, approaching a nearly constant value. The contribution due to convection is considered to be small, therefore, the heat transfer coefficient is taken to be constant as 2.6×10^{-2} and 3.6×10^{-2} kW m^{-2} K^{-1} for the cases of PMMA and red oak burning, respectively.

Defining the dimensionless temperature θ as $(T - T_i)/T_i$, solution of equations (17) and (18) can be readily obtained using the Laplace transform method as [12]

$$\theta(x, t) = \frac{\varepsilon_s q_p}{T_i h} - \left\{ \operatorname{erfc}\left(\frac{x}{2\sqrt{\alpha t}}\right) - \exp\left(\frac{hx}{\lambda} + \frac{\alpha h^2 t}{\lambda^2}\right) \times \operatorname{erfc}\left(\frac{x}{2\sqrt{\alpha t}} + \frac{h\sqrt{\alpha t}}{\lambda}\right) \right\} \tag{19}$$

where erfc(x) is the complementary error function. If the effect of in-depth absorption, with the assumption of Arrhenius-type chemical reactions, is considered, the energy equation for the solid may be expressed as [13]

$$\frac{\partial \theta}{\partial t^*} = \frac{\partial^2 \theta}{\partial x^{*2}} + A \exp(-E^*/\theta) \tag{20}$$

where E^* denotes a dimensionless activation energy defined as E/RT_i. Another dimensionless parameter A measures the relative importance of chemical and external (radiative) heating and will be found later. This differs from the analysis due to the thermal theory of ignition and is often employed in solid propellant ignition where overall exothermic reactions take place both in the gas phase and in the solid phase. During the ignition delay period of plastic fuels, endothermic solid-phase reactions, such as surface charring, are observed. This type of heat sink effect, however, has been shown to be insignificant, since the total amount of pyrolysis is so small that the endothermicity has little effect during the ignition delay period [10]. It is interesting to note that as the ignition delay period is prolonged, the effect of endothermic pyrolysis becomes important [8]. Alternatively, equation (20) can be rewritten as

$$\frac{\partial \theta}{\partial t^*} = \frac{\partial^2 \theta}{\partial x^{*2}} + \exp\left\{\left(\frac{E^*}{\theta_c}\right)\left(\frac{\theta - \theta_c}{\theta}\right)\right\} \tag{21}$$

where A is defined as $\exp(E^*/\theta_c)$. Equation (21) implies that in the limit of large activation energy, namely $E^*/\theta_c \to \infty$, the reaction rate term will be exponentially small for $\theta < \theta_c$, and exponentially large for $\theta > \theta_c$. For the lowest order of the small parameter θ_c/E^*, if the characteristic time t^* is small enough to assure that $\theta < \theta_c$ everywhere in the solid, then equation (21) reduces to equation (17). Thus, the energy equation for the reactive solid becomes identical to that of an inert solid, to the lowest order.

The temperature given by equation (19) monotonically decreases with x, and monotonically increases with t, therefore, the lowest order (inert solid) approximation will break down earliest at the fuel surface, $x = 0$. From equation (21), the reaction rate increases exponentially for $\theta(0, t) > \theta_c$. It is thus clear that to the lowest order in θ_c/E^*, the quantity θ_c represents an ignition temperature at which thermal runaway occurs. Therefore, the ignition temperature is given by

$$\theta_{ig} = \frac{\varepsilon_s q_R}{T_i h}\left\{1 - \exp\left(\frac{\alpha h^2}{\lambda^2} t_{ig}\right) \operatorname{erfc}\left(\frac{h}{\lambda}\sqrt{\alpha t_{ig}}\right)\right\}. \tag{22}$$

In the present analysis, higher-order effects are included using the empirical results obtained by Bradley [13]. He has found that for the reactive solid fuels, the ignition temperature, θ_{ig}, and ignition delay time, t^*_{ig}, are related as

$$\theta_{ig} = 1 + 1.3(t^*_{ig})^{1/2}. \tag{23}$$

The surface temperature at time t^*_{ig} for an inert solid is obtained as

$$\theta_s = 1 + 2(t^*_{ig}/\pi)^{1/2}. \tag{24}$$

Combining equations (23) and (24) gives

$$(\theta_{ig} - 1)/(\theta_s - 1) = 1.16. \tag{25}$$

This implies that the surface temperature rise of the reactive solid fuels must be 16% higher than the surface temperature rise of an inert solid for ignition to occur. The ignition delay time in the present analysis is based on $1.16\theta_s$, in order to include higher-order analyses.

3. RESULTS AND DISCUSSION

Ignition delay times as a function of radiative heat flux for PMMA and red oak fuels are shown in Figs. 2 and 3. Comparisons are made with the experimental data [3, 11] for cases with and without blockage effects. Kashiwagi measured ignition delay times vs radiative heat flux, but did not measure, in detail, the concentration of the gases. His ignition data were based on absorption through a rising plume of evolved gases under a no-flame condition. It is expected that the composition of these gases will not differ significantly from the products of combustion. To make a comparison between the present analysis and his experiment, three different layer compositions are postulated. One case considers the absorption–emission process when soot particles are the dominant contributing elements. Based on many previous experimental observations [14], the absorption coefficient is taken as 1.3 m^{-1} in this case. The second examines the opposite extreme where a hydrocarbon gas mixture is primarily responsible for the attenuation of radiation. The third is the case of $k = 0$, which is obviously the case of no blockage of thermal radiation. Also, the present model illustrated in Fig. 1 is thought to be closer to pilot ignition situations due to the presence of a flame maintained at the side walls. Thus predictions are compared with pilot ignition data. In the combustion of PMMA, some of the important hydrocarbon gas species evolved from the fuel surface are propylene (C_3H_6), ethylene (C_2H_4), methane (CH_4) and acetylene (C_2H_2). Mole fractions of these species are generally very small, ranging from 0.002 to 0.005 [15], thus individual contributions of each element are minor. However, as a mixture, the contribution from these constituents could be significant over the infrared spectral range due to the filling of the absorption band window regions by the other species [4]. The other major constituent is the monomer ($C_5H_8O_2$) with a mole fraction range from 0.03 to 0.05. The absorption coefficient of a mixture of hydrocarbon gases and the monomer is taken as 0.2 m^{-1}, assuming that the contribution from each constituent is superposable, and that each element has an absorption coefficient the same order of magnitude of methane (CH_4) at 1 atm and 1000 K.

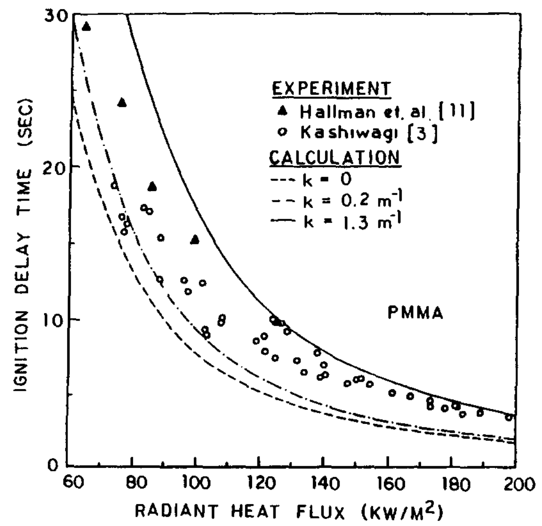

FIG. 2. Ignition delay time as a function of radiative heat fluxes for PMMA.

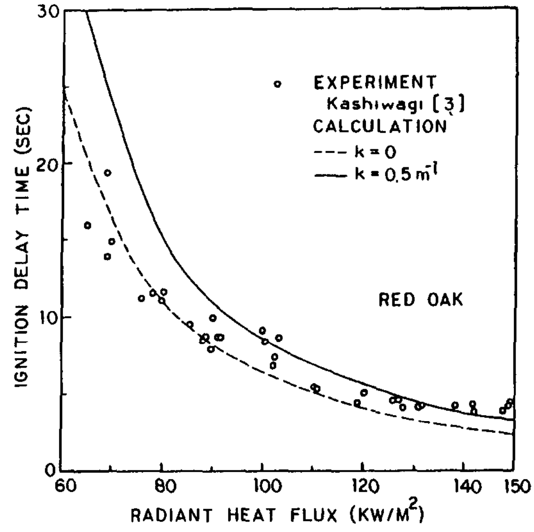

FIG. 3. Ignition delay time as a function of radiative heat fluxes for red oak.

Figure 2 shows that for lower heat fluxes, the calculation with $k = 0.2\ m^{-1}$ agrees well with the experiment and for higher heat fluxes $k = 1.3\ m^{-1}$ gives good agreement. This indicates that the hydrocarbon gas mixture and monomer may be the primary elements responsible for the radiative attenuation in lower heat flux ranges. As the heat flux increases, carbon particulates are more likely to be generated from the solid fuel surface, becoming the dominant element for the attenuation of radiative heat. These carbon particulates can possibly be generated even in a no-flame condition, as observed in smouldering phenomena. Over the entire heat flux range, the discrepancy between the present analysis and experiment is partly due to the assumption of constant absorption coefficient. For lower heat fluxes, the gas layer formed by decomposition products is thinner and less sooty than for higher heat fluxes, and the blockage effect is small. Consequently, the calculation tends to overpredict the blockage effect for lower heat flux ranges. This will result in an overestimation of ignition delay time. As heat flux increases, decomposition of the solid fuel occurs at a faster rate, forming a thicker and sootier layer. Thermophysical properties used in the calculations are thermal conductivity λ ($kW\ m^{-1}K^{-1}$) $= 1.9 \times 10^{-4}$ (PMMA) and 1.5×10^{-4} (red oak), density ρ ($kg\ m^{-3}$) $= 1200$ (PMMA) and 700 (red oak),

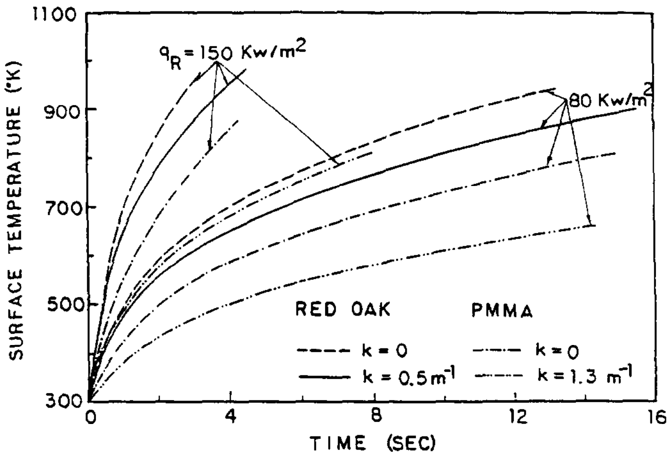

FIG. 4. Fuel surface temperature history for various radiative heat fluxes for PMMA and red oak.

specific heat c (kJ kg^{-1} K^{-1}) = 1.4 (PMMA and red oak), respectively. For red oak, in lower heat flux range up to 100 kW m^{-2}, experimental data agree well with the case of no-blockage, as can be seen in Fig. 3. This is primarily due to the fact that the blockage effect becomes less significant for the prolonged ignition delay period, and also due to the fact that the composition of pyrolyzed gases is effectively transparent. Unlike plastic fuels, decomposition products from wood in the lower heat flux ranges are not hydrocarbon gases, which block radiation quite considerably. As the heat flux reaching the wood surface increases, soot can be generated during the ignition delay period, thus the effect of radiation blockage begins to play an important role. Consequently, calculated ignition delay times are in better agreement with experimental data in the higher heat flux range. In the calculation for red oak, k is taken to be 0.5 m^{-1} based on experiment [1].

In Fig. 4, calculated solid fuel surface temperature histories for various radiative heat fluxes with and without the blockage effect are shown. It can be seen that the blockage effect is more pronounced for PMMA than for red oak. In general, the blockage effect is more significant for sootier fuels than the relatively clean fuels, as should be expected. This generalization is clearly seen in Fig. 5, which depicts the relation between ignition delay time and radiative heat fluxes on a nondimensional basis. Since the soot content of PS fuels are usually a factor of 5–10 greater than PMMA fuels [6], blockage effects are more significant for PS than PMMA fuels.

Many different ignition criteria have so far been proposed and a summary of various ignition criteria can be found in ref. [16]. Two of the most common ignition criteria are the heat balance criterion and the temperature criterion. By comparing these two ignition criteria, Bradley has found that they can be correlated within 4% accuracy as a single criterion [13]. Following his result, ignition delay time and heat

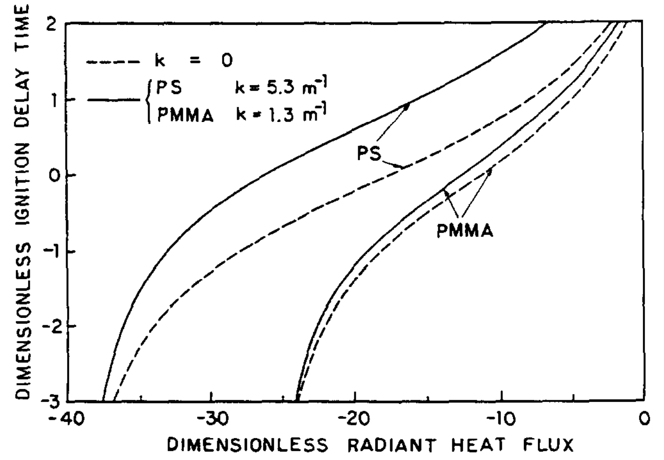

FIG. 5. Relationship between heat fluxes and ignition delay time for PMMA and PS fuels.

flux are related, on a nondimensional basis, as

$$A = \frac{H\nu\lambda T_i}{q_R^2} = \frac{\sqrt{E^*}(\pi t_{ig}^*)^{-1/4}}{(1+2\sqrt{t_{ig}^*/\pi})} \exp\{E^*/(1+2\sqrt{t_{ig}^*/\pi})\} \quad (26)$$

where ν and H are the frequency factor and the heat of reaction, respectively. For comparison purposes, the abscissa of Fig. 5 is taken to be $\log_{10}(1/A)$ which corresponds to that of Bradley. As the value of the abscissa decreases, the actual heat flux increases. Input values used in the calculations are: the activation energy E (kJ mole^{-1}) = 134 (PMMA) and 209 (PS), the frequency factor ν (s^{-1}) = 10^{10} (PMMA) and 10^{14} (PS), and the heat of reaction H (kJ kg^{-1}) = 2.5×10^4 (PMMA) and 4×10^4 (PS), respectively. These are the averaged values, since they differ, in some cases, by a factor of 2 depending on the sources [17–21]. From Fig. 5, it can be clearly seen that the blockage effect on the ignition delay time may become significant for sootier fuels such as PS, and that as the heat flux decreases the blockage effect becomes significant. It is obvious that the calculated ignition delay time without blockage in a room fire will result in a considerable error for sootier ceiling materials.

4. CONCLUSION

The effect of radiation blockage due to the smoke ceiling layer on ignition delay time and thermal behaviors of reactive condensed fuels have been studied through a simplified model. Applicability of the present analysis has been demonstrated. Important physical trends and findings noted in this analysis can be summarized as follows.

1. Inclusion of radiation blockage leads to more accurate determination of surface temperature variations and ignition delay times when the layer of decomposition is present in room fire situations.
2. Using the existing ignition theory, composition of evolved gases in the smoke layer during the ignition delay period could be estimated by comparing experiments with calculations by known absorption coefficients.
3. The effect of radiation blockage is more significant for sootier fuels such as PS and neglecting the effect of blockage due to the ceiling layer above the fuel surface will result in an underestimation of ignition delay times.
4. For the same smoke layer thickness, the effect of blockage becomes less significant as the heat flux increases.

Acknowledgment—This work was supported by the Center for Fire Research of the National Bureau of Standards, U.S. Department of Commerce.

REFERENCES

1. J. G. Quintiere, The growth of fire in building compartment, ASTM–NBS Symposium on Fire Standard and Safety, Preprint No. 7 (1976).
2. J. G. Quintiere and B. J. McCaffrey, The burning of wood and plastic cribs in an enclosure, NBSIR 80-2054, Vol. 1 (1980).
3. T. Kashiwagi, Experimental observation of radiative ignition mechanisms, *Combust. Flame* **34**, 231–244 (1979).
4. K. Y. Lee, Z. Y. Zhong and C. L. Tien, Blockage of thermal radiation due to soot layer in combustion of condensed fuels, *Twentieth Symposium (International) on Combustion*. The Combustion Institute, in press.
5. T. Kashiwagi, B. W. Macdonald, H. Isoda and M. Summerfield, Ignition of a Solid Polymeric Fuel in Hot Oxidizing Gas Stream, *Thirteenth Symposium (International) on Combustion*, pp. 1073–1086. The Combustion Institute (1970).
6. G. L. Hubbard and C. L. Tien, Infrared mean absorption coefficients of luminous flames and smoke, *J. Heat Transfer* **100**, 235–239 (1978).
7. E. M. Sparrow and R. D. Cess, *Radiation Heat Transfer*, Chap. 8. McGraw-Hill, New York (1978).
8. F. R. S. Clark, Ignition of poly(methyl methacrylate) slabs using a small flame, *J. Polymer Sci., chem. Ed.* **22**, 2323–2334 (1983).
9. T. J. Ohlemiller and M. Summerfield, Radiative ignition of polymeric materials in oxygen/nitrogen mixtures, *Thirteenth Symposium (International) on Combustion*, pp. 1087–1094. The Combustion Institute (1970).
10. T. Kashiwagi, A radiative ignition model of a solid fuel, *Combust. Sci. Technol.* **8**, 225–236 (1974).
11. J. Hallman, J. R. Welker and C. M. Sliepcevich, Ignition of polymers, *SPE J.* **28**, 43–47 (1972).
12. H. S. Carlslaw and J. C. Jaeger, *Conduction of Heat in Solids*, 2nd edn. Oxford University Press, Oxford (1959).
13. H. H. Bradley, Theory of ignition of a reactive solid by constant energy flux, *Combust. Sci. Technol.* **2**, 11–20 (1970).
14. J. De Ris, Fire radiation—a review, *Seventeenth Symposium (International) on Combustion*, pp. 1003–1016. The Combustion Institute (1979).
15. K. Sheshadri and F. A. Williams, Structure and extinction of counterflow diffusion flames above condensed fuels: comparison between poly(methyl methacrylate) and its liquid monomer, both burning in nitrogen–air mixtures, *J. Polymer Sci., chem. Ed.* **16**, 1755–1778 (1978).
16. K. Annamalai and P. Dubertaki, Ignition of thermally thin porous pyrolyzing solids under normally impinging flames, *Combust. Flame* **27**, 253–266 (1976).
17. L. A. Wall, Pyrolysis of polymers, NBS-SP No. 357, *Proc. 4th Material Research Symposium*, pp. 47–60 (1970).
18. F. J. Martin, A model for the candle-like burning of polymers, *Combust. Flame* **12**, 125–135 (1968).
19. G. A. Legelle, Thermal degradation kinetics and surface pyrolysis of vinyl polymers, *AIAA Jl* **8**, 1989–1996 (1960).
20. M. Gordon, Probability model theory of chain-end active polymer degradation, III, statistical kinetics of degradation of polymethyl methacrylate, *J. phys. Chem.* **64**, 19–29 (1960).
21. F. R. S. Clark, The role of oxygen in the ignition of polystyrene by a small flame, *J. Polymer Sci., chem. Ed.* **22**, 263–268 (1984).

IGNITION DE COMBUSTIBLE PAR RAYONNEMENT DANS UN FEU DE PLAFOND EN INCLUANT LES EFFETS DE BLOCAGE RADIATIF

Résumé—On étudie les effets de blocage du rayonnement thermique dûs à une couche absorbante et émettrice formée sous le toit pour une ignition de matériaux. L'analyse utilise un modèle relativement souple mais réaliste dans des conditions monodimensionnelles et stationnaires. Les temps de mise à feu s'accordent avec les données expérimentales et l'histoire thermique du plancher influencée par le blocage radiatif. Des formules générales entre les temps d'ignition et les flux thermiques radiatifs sont obtenus pour des combustibles polymères typiques comme PMMA et PS, et on discute de l'application de cette analyse.

DURCH STRAHLUNG VERURSACHTE ENTZÜNDUNG VON KONDENSIERTEN BRENNSTOFFEN BEI DECKENFEUER UND DER EINFLUSS EINER STRAHLUNGSUNTERBRECHUNG

Zusammenfassung—Der Einfluß der Strahlungsunterbrechung durch eine absorbierend-emittierende Schicht unter der Decke auf die Entzündung von Bodenmaterialien wird untersucht. Die Arbeit vermittelt ein relativ einfaches aber realistisches Modell unter eindimensionalen quasistationären Bedingungen. Der berechnete zeitliche Verzug bis zur Entzündung stimmt gut mit experimentellen Daten überein; es ergibt sich der zeitliche Temperaturverlauf am Boden unter Einwirkung der Strahlungsunterbrechung. Allgemein gültige Beziehungen zwischen der Zeit bis zur Entzündung und der Wärmestromdichte durch Strahlung werden für typische Polymer-Brennstoffe wie PMMA und PS ermittelt. Die Anwendbarkeit der vorgelegten Untersuchung wird diskutiert.

РАДИАЦИОННОЕ ВОСПЛАМЕНЕНИЕ КОНЦЕНСИРОВАННОГО ТОПЛИВА ОТ ОГНЯ ПОД ПОТОЛКОМ, ВКЛЮЧАЯ ЭФФЕКТЫ БЛОКИРОВАНИЯ ИЗЛУЧЕНИЯ

Аннотация—Изучается влияние блокирования теплового излучения за счет поглощающего-излучающего слоя под потолком на воспламенение материалов пола. Использована относительно простая одномерная и квазистационарная реалистичная модель. Рассчитанные времена задержки воспламенения сравниваются с экспериментальными данными; получена временная эволюция температуры пола под влиянием блокирования излучения. Получены зависимости времен задержки воспламенения от радиационных тепловых потоков для типичных полимерных топлив, таких как PMMA и PS. Обсуждаются границы применимости данной модели.